SINGLE- AND DOUBLE-PULSED HOLOGRAPHY FOR THE CHARACTERIZATION OF SPRAYS OF REFRIGERANT R113 INJECTED INTO ITS OWN SATURATED VAPOR

A. Chávez, F. Mayinger

Lehrstuhl A für Thermodynamik, Technische Universität München
Arcisstr. 21, 8000 München 2, FRG

ABSTRACT

A holographic study of sprays of liquid refrigerant R113 injected into its own saturated vapor is presented. The experiments were carried out in a thermally insulated autoclave, at different liquid mass flow rates $\dot{m}$ (32.50 – 231.87 g/min) and vapor pressures p_v (0.10 – 0.25 MPa). For each combination of $\dot{m}$ and p_v, two holograms were recorded – a single-pulsed hologram to provide data about spray angle, break-up length and drop size distribution, and a double-pulsed one to evaluate the drop velocities – . The results were compared with data obtained from the literature of water sprays in steam environments and the differences discussed.

1. INTRODUCTION

The knowledge about the behaviour of sprays injected into condensable environments (i.e. into its own vapor) is important for the correct design of industrial processes and for better understanding of dispersed fluid phenomena.

Over the years, numerous research has been carried out on sprays dealing with their formation and with the evaluation of droplet parameters. These include stability and desintegration of liquid sheets *Dombrowski & Johns* [1], effect of ambient and liquid properties *De Corso & Kemeny* [2]; *De Corso* [3]; *Dombrowski & Hooper* [4], atomization and nozzle design *Mugele & Evans* [5], *Fraser & Eisenklam* [6]; *Kim & Marshall* [7]; *Dombrowski & Wolfsohn* [8]. The different measurement methods employed were presented in an extensive review by *Azzopardi* [9].

In the last few years, the perfection of the laser technique made the application of more powerful non-intrusive methods possible to study dispersed flows. Two major areas have been developed: on one side, the LDA-sizers which base on the analysis of LDA signals, as is decribed in the studies of *Durst & Eliasson* [10]; *Swithebank, et al* [11]; *Yule, et al* [12]; *Farmer* [13]; *Baukhage* [14]; *and Bachalo* [15]; on the other side, pulsed laser holography which bases on the Gabor-Holography *Gabor* [16], as illustrated in the reviews of *Thompson* [17] and *Trollinger* [18, 19]. These two groups of measuring methods seem to be the most appropriate to provide spray information for the range of drop diameters $10\lambda < d < 3$ mm, where λ is the wavelength of the laser light.

In this work, we applied pulsed laser holography for direct measurement of size and velocity distributions of spray droplets of the liquid refrigerant R113 (Trifluorotrichloroethane), and for the characterization of the spray. The physical properties of the refrigerant R113 allow to carry out direct contact condensation experiments in a wide field of reduced pressures ($p_r = p_v/p_c$) in a technical, favorable range of pressure and temperature (T_c = 214.1 °C; p_c = 3.41 MPa). This characteristic can help us to overcome the difficulty of conducting water-steam experiments at high reduced pressures by providing generalized spray-correlations. Here p_v is the vapor pressure of the spray environment and p_c and T_c are the critical pressure and temperature respectively.

Experimental Heat Transfer, Fluid Mechanics, and Thermodynamics 1988
R.K. Shah, E.N. Ganić, and K.T. Yang, Editors

2. SCOPE OF THE WORK AND SPRAY DESCRIPTION

In this paper, results of a holographic evaluation of R113-spray experiments realized for the range of vapor presures p_v (0.10 – 0.25 MPa) and liquid mass flow rates $\dot{m}$ (32.5 - 231.87 g/min) according to the experimental matrix shown in Table 1 are presented. A common hollow-cone type swirl nozzle (Lechler Co.) with a diameter of 0.7 mm was used as an atomizer.

A schematic picture of the spray flow is shown in Fig.1. Assuming that the spray possesses a steady axis, we can use cylindrical polar coordinates to relate the spray with spacial positions; here the axis z of the coordinate system coincides with the spray axis and the origin is situated at the outlet of the nozzle. The spray may be divided into three zones: the continuous liquid sheet zone, the break-up zone and the droplet zone. The form of the liquid sheet – characterized by the spray angle α and the break-up length Lz – plays an important role; it is responsible for the final form of the spray. At the distance Lz, the liquid sheet becomes unstable – aerodynamic instability – and it breaks up into a swarm of fine droples. Due to this unstable break-up mechanism, the produced drops are of very different sizes and fly at different velocities. This can be taken into account by setting up distributions of size and velocity with respect to the reference frame.

Summarizing: in order to describe the spray, measurements of the shape and length of the liquid sheet and of the size and velocity distributions of the droplets are necessary.

Table 1. Experimental Matrix

$\dot{m}$ (g/min)	p_v (MPa) 0.10	0.15	0.20	0.25
32.50	x			
64.44	x	x	x	x
82.28	x			
101.86	x			
141.66	x			
231.87	x			

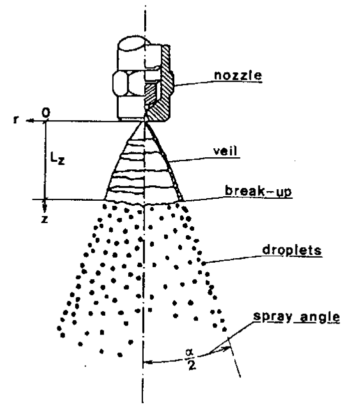

Fig.1 Schematic diagram of the spray flow.

3. MEASURING TECHNIQUE

3.1 Pulsed Laser Holography

For direct measurement of the spray parameters, we decided to apply the pulsed laser holography. It is a well-tested measuring method for single-pulsed holograms (*Hawighorst* [20], *Timko* [21]) and with the use of a multi-pulsed ruby laser, direct measurement of droplet velocities are also possible. Holography permits storing a high-resolution, three- dimensional image of the whole particle field at any instant. The frozen image of the particle field can then be analysed in detail, through its volume, with conventional imaging systems.

In the present study, conventional single pulsed laser holography (where a single exposure was made with one firing of the ruby laser) was carried out to measure the drop sizes and to observe the spray form. Next, double-pulsed laser holography (where a double exposure was made with two firings at a pulse interval of 200 μs of the ruby laser) was employed to obtain the droplet velocities. Typical photographs of single- and double-pulsed holograms are shown in Figs. 2 and 3 respectively.

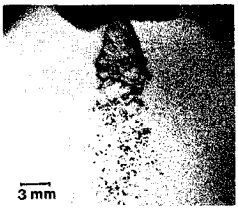

Fig.2 Photographs of a single-pulsed hologram for the measurement of the break-up length, spray angle, and drop size.

Pulse energy: 1 Joule
Pulse duration: 30 ns
$\dot{m} = 64.44$ g/min ; $p_v = 0.15$ MPa

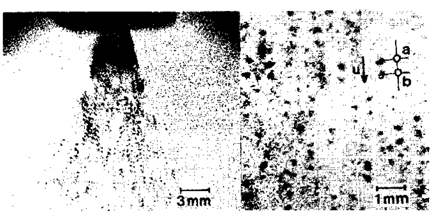

$$u = \frac{b-a}{\text{Pulse Interval}}$$

Fig.3 Photographs of a double-pulsed hologram for the evaluation of the drop velocities.

Pulse energy: 0.5 Joule
Pulse duration: 30 ns
Pulse interval: 200 μs
$\dot{m} = 64.44$ g/min ; $p_v = 0.15$ MPa

3.2 Holographic System

3.2.1 Arrangement for the recording of the holograms. The layout of the holographic system with the autoclave wherein the spray is produced is shown in Fig.4. An off axis arrangement using a pulsed ruby laser (K-Lasers Ltd.) was employed. The laser produces light of a wavelength of 694.3 nm, with an output energy of 1 J and a pulse width of 30 ns. It can also be operated in double-pulse modus with pulses of 0.5 J at intervals from 1 to 800 μs. A convex lens **DL** was used to expand the laser beam at the entrance of the holographic

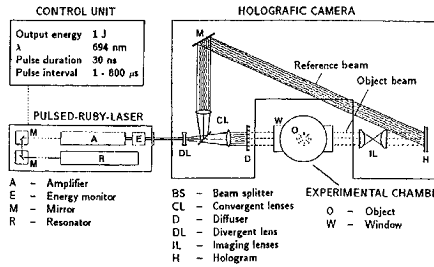

Fig.4 Arrangement for recording holograms.

arrangement to reduce the power concentration, and a beamsplitter **BS** to produce two beams, the so-called object and reference beam. The beams were collimated by the lenses **CL** to obtain parallel beams of 60 mm diameter. The object beam is then led into the experimental chamber through the diffusor **D** which provides uniform illumination of the object **O** and is transmitted through the spray. Imaging lenses **IL** were placed between the spray and the holographic plate (Agfa 8E75 HD). These lenses provide a conjugate image of the spray close to the holographic plate and reduce the necessity of the hologram to achieve a high resolution. The reference beam was reflected by the mirror M to the holographic plate where it combined with the object beam. The position of the mirror M was adjusted so that the optical path difference between the reference and the object beam path was kept shorter than the laser coherence length ($\sim$ 20 cm). The exposed holographic plates were developed and bleached according to standard formulas, for example *Hariharan* [22].

3.2.2 Arrangement for the reconstruction of the holograms. The reconstructed image of the liquid spray was obtained by illuminating the developed holographic plates – holograms – with a continuous Helium-Neon (He-Ne) laser beam which replaced the reference beam. Figure 5 shows the optical arrangement for taking photographs of the virtual image of the reconstructed hologram. By turning the plate 180°, a real image is produced which can be photographed directly with microscope objectives.

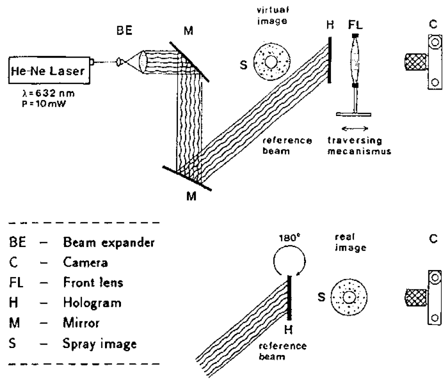

Fig.5 Reconstruction of the holograms.

<u>3.2.3 Evaluation of the holograms.</u> The holograms were evaluated by a manual method. First, a series of photographs was taken from each hologram in which the focussing length was stepwise varied by adjusting the camera lenses, sweeping the full depth of the holographic image, as shown schematically in Fig.5. By this method the three-dimensional information of the hologram was converted into a set of two dimensional slides (photographs) containing the part of the hologram information corresponding to the focal plane at which the photograph was recorded. The photographs could then be evaluated easier. The focussing depth of the photographs was kept as short as possible using a 400 mm teleobjective and a 500 mm front-lens which was moved to shift from a focal plane to another. Taking the pictures with this procedure, alterations in size due to optical aberrations could be neglected. To assure correct measurements, only very well focussed droplets, selected by human criterion, were taken into account.

To measure the recorded pictures, the film negatives were projected onto a translucent screen measuring 130 cm x 100 cm using a common slide projector. The projected images could then be directly measured with a calibrated magnifier. Total magnifications up to 100 : 1 were achieved. A holographic image of a tungsten wire of 100 μm diameter was used as a calibration scale. The Fig. 6 shows a series of droplet pictures – corresponding to the same reconstructed hologram – taken at different focal planes. It can be seen that the droplets appear well focussed only in one of the focal planes.

4. EXPERIMENTAL APPARATUS AND PROCEDURE

4.1 Test Chamber

Figure 7 shows a schematic diagram of the thermally insulated pressure vessel, which was used as the test chamber. It consists of a cylinder measuring 206 mm in interior diameter and 650 mm in hight. It was designed for pressures up

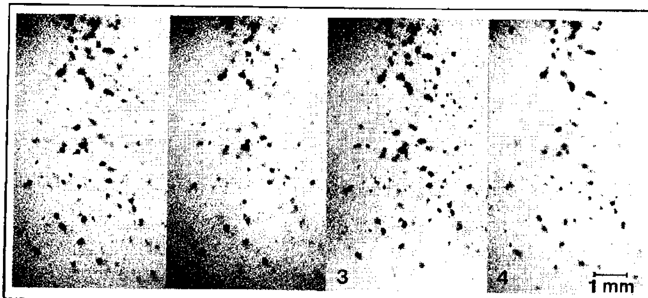

Depth interval between two pictures: $\sim$ 1 mm
p_v = 0.1 MPa
$\dot{m}$ = 32.50 g/min

Fig.6 Photographs of the R113-spray taken at different focal planes of the reconstructed image of a single-pulsed hologram.

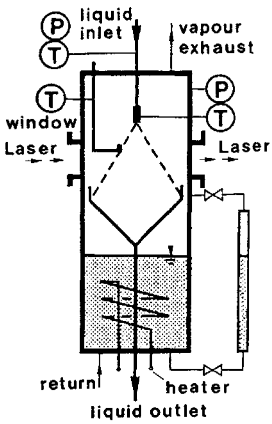

Fig.7 Schematic diagram of the test chamber.

to 2 MPa. Two quartz glass windows having 100 mm in diameter were installed in the cylindrical wall for optical access. The spray was injected from the top of the vessel through the fine hollow cone nozzle described in section 2, which was positioned concentric with respect to the cylindrical wall. Its position can be axially varied to permit the observation of any section of the spray. The lower third of the vessel was filled with liquid refrigerant R113 which was heated by three electrical heating elements (1.2 kW) installed in the lower plenum, to produce the saturated vapor environment in the upper two thirds of the vessel. A funnel was placed between the boiling liquid and the spray. It collected the spray droplets and led them to the outlet.

4.2 Facility

The liquid to be injected into the test chamber was supplied by a R113-reservoir, maintained at high pressure by connecting it to a pressurizer. The hot liquid, drained from the test chamber, was cooled down to the room temperature by a water cooler and finally led to the storage tank, as indicated in the flow diagram in Fig. 8. The liquid flow rate supplied to the nozzle was measured with a finely calibrated rotameter (Fischer & Porter) and kept constant for each run. The temperature and pressure at points of interest in the test chamber were monitored with conventional thermocouples and pressure sensors connected to a central indicator.

4.3 Experiment

The vapor which is generated in the test chamber is maintained at the experiment pressure by regulating a relief valve. Liquid is supplied to the nozzle at a pre-established mass flow rate and temperature. Experiments were conducted at a liquid temperature T_l of 25 °C. The mass flow rate $\dot{m}$ and the vapor pressure p_v were varied according to the experimental matrix shown in Table 1. For each combination of $\dot{m}$ and p_v, at steady-state conditions, two holograms were taken: a single-pulsed hologram to provide data about spray angle, break-up length and drop size distribution, and a double-pulsed one to evaluate the drop velocities. Two series of experiments were conducted:

- first, the vapor pressure was maintained constant at 0.10 MPa while the liquid mass flow rate was varied from 32.50 – 231.87 g/min.
- next, the mass flow rate was kept constant at 64.44 g/min while the vapor pressure was varied from 0.15 – 0.25 MPa.

In the first case the results (Table 2) showed a strongly dependence of the drop size, drop velocities, spray angle and breakup length upon the

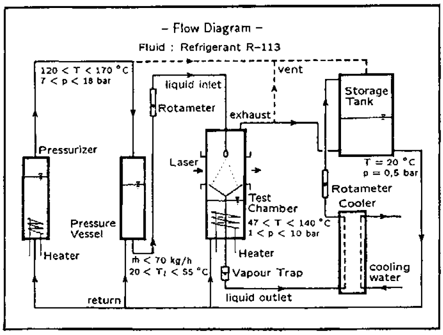

Fig.8 Test Facility for conducting R113-spray experiments.

mass flow rate, as can be appreciate in the diagrams of Fig.9. As an illustration, Fig.10 shows a series of photographs of reconstructed holograms. In the second case, the results (Table 3) indicated only a weakly decreasing of the spray angle and drop sizes while the vapor pressure was increased. The result of this series are presented in the diagrams of Fig.11.

The measurements of the breakup length were compared with spray-correlations obtained from the literature, which were produced from experiments conducted on water-sprays injected into steam environments. This indicated that R113-sprays can not be directly described with this kind of correlations. For example, Fig. 12 shows a plot of the a spray correlation from *Lee & Tankin* [23] (for p_r < 0.014) in which the results of this

Table 2. Results of experiments for p_v = 0.1 MPa

$\dot{m}$ (g/min)	r (mm)	z (mm)	$\bar{d}$ (μm)	d_{max} (μm)	d_{min} (μm)	$\bar{u}$ (m/s)	Lz (mm)	α
	0.50	3.48	340	450	220		3.48	25.6
32.50	1.14	5.70	380	540	220	0.70		
	2.28	11.40	370	570	170	0.70		
	2.16	5.70	310	340	220		5.70	30.8
64.44	2.26	11.40	370	450	310	1.66		
	3.64	17.10	370	420	310	1.66		
	3.10	5.30	290	340	205		5.30	66.0
82.28	6.35	11.40	250	280	230	2.50		
	14.20	17.10	290	350	250	2.50		
	3.02	5.13	230	235	230		5.30	66.0
101.86	6.30	11.70	240	285	190	3.35		
	17.80	17.10	269	310	199	3.35		
	4.10	3.75	240	290	182		3.75	71.6
141.66	8.21	11.40	130	140	110	3.75		
	11.17	17.10	140	190	90	3.75		
	3.30	2.40	150	190	110		2.40	72.0
231.87	7.52	11.40	100	140	50	5.02		
	10.90	17.10	120	140	90	5.02		

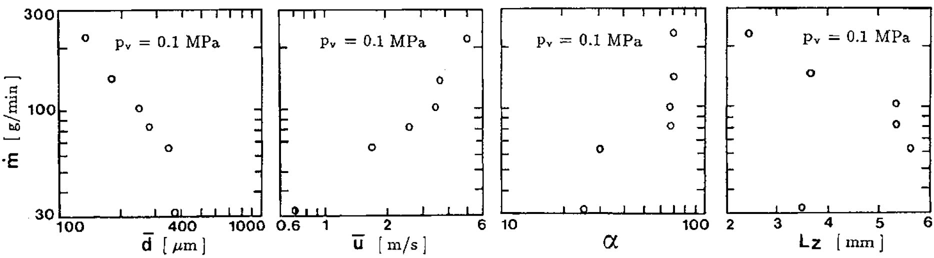

Fig.9 Mean drop diameter, velocity, spray angle and break-up length vs. the mass flow rate.

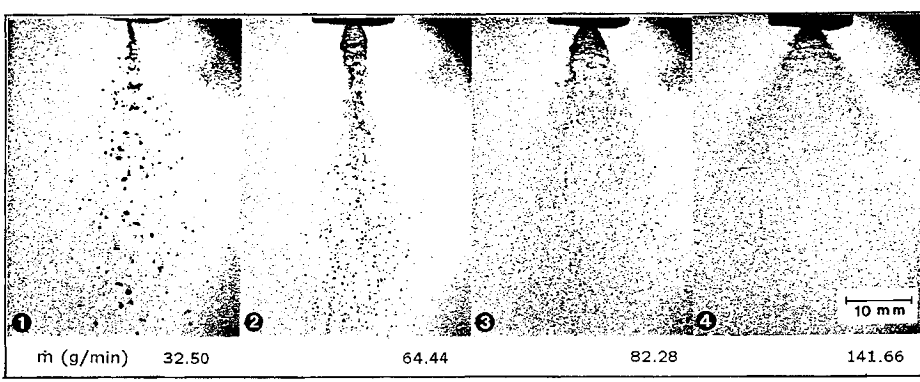

Fig.10 Photographs of the R113-spray at different mass flow rates. Object: R113-spray in its own saturated vapour at 0.1 MPa Pulse energy: 1 Joule ; Pulse duration: 30 ns

work were also included. The behavioural discrepancies can be cleared through the strong differences in the physical properties of water and refrigerant R113. The surface tension σ, the viscosity μ and the liquid density ρ play a determinating role. For example for $p/p_c < 0.3$, the properties of the refrigerant R113 and water (H_2O) obey the following relations $\sigma_{R113} \sim \sigma_{H_2O}/3$, $\mu_{R113} \sim 2.7\,\mu_{H_2O}$ and $\rho_{R113} \sim 1.7\,\rho_{H_2O}$ respectively.

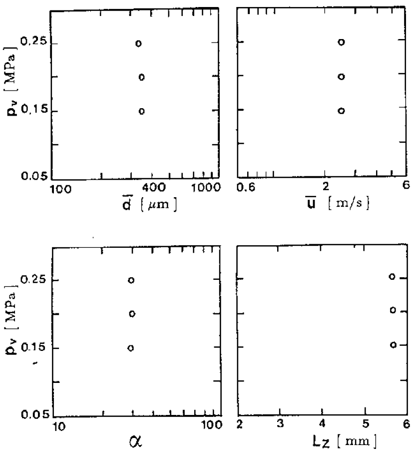

Fig.11 Mean drop diameter, mean drop velocity, spray angle and break-up length vs. the vapor pressure for $\dot{m}$ = 64.44 g/min.

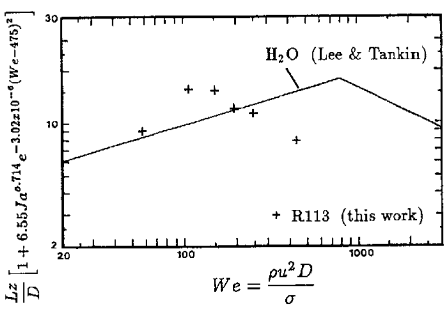

Fig.12 Breakup length of the liquid sheet as a function of Weber and Jakob numbers.

Table 3. Results of experiments for $\dot{m}$=64.44 g/min

p_v (MPa)	r (mm)	z (mm)	$\bar{d}$ (μm)	d_{max} (μm)	d_{min} (μm)	$\bar{u}$ (m/s)	Lz (mm)	α
	2.12	5.70	310	330	220		5.70	29.8
0.15	2.30	11.40	360	450	300	1.66		
	3.60	17.10	360	420	300	1.66		
	2.10	5.70	310	340	220		5.70	29.2
0.20	2.30	11.40	360	430	300	1.66		
	3.60	17.10	360	420	300	1.66		
	2.10	5.70	310	340	220		5.70	29.2
0.25	2.30	11.40	360	430	300	1.66		
	3.60	17.10	350	420	280	1.66		

4.4 Uncertanty Sources

The human criterion in our hologram's evaluation method, especially to decide whether a droplet appears sharp enought in the photographs, is a dominant factor in the estimation of the uncertanties of the results. In order to take into account this error source, three persons evaluated separately the film negatives corresponding to all the holograms reported here and their measurements were compared together. Deviations up to 16% were achieved. Errors due to other sources were one order of magnitude smaller.

5. SUMMARY

Both single- and double-pulsed holograms were very clear and could be photographed relatively easy . The spray parameters were then evaluated from the photographs for some interesting spray zones, and the results summarized in Tables 2 and 3. The results showed that the dropsize is inversely proportional to both the mass flow rate and vapor pressure while the dropsize and velocity distributions, spray angle and breakup length depend only weakly upon the vapor pressure and very strongly upon the mass flow rate, as indicated in the photographic series of Fig.10. Moreover, they revealed that refrigerant sprays can not be directly described by usual correlations which were obtained from water-steam experiments. In spite of this it seems promising, that with sufficient R113-spray data, it will not be very difficult to extend actual spray-correlations – or to provide new, more general correlations – in future research, to predict the behaviour of generalized sprays for higher reduced pressures.

Acknowledgements. ACh thanks the mexican Instituto de Investigaciones Electricas and CONACYT, the Deutsche Forschungsgemeinschaft and the Lehrstuhl A für Thermodynamik of the Tech. Universität München for the financial support for this study.

NOMENCLATURE

D_n	nozzle diameter	[mm]
Cp	specific heat	[kJ/kg K]
Lz	break-up length	[mm]
Ja	Jakob number Ja = Cp (Ts - T)	[-]
O	origin of coordinates	[-]
T	temperature	[°C]
We	Weber number $We = \rho u^2 D_n / \sigma$	[-]
d	droplet diameter	[μm]
$\bar{d}$	mean droplet diameter	[μm]
h	heat of vaporization	[kJ/kg]
$\dot{m}$	liquid mass flow rate	[g/min]
p	pressure	[MPa]
r	radial coordinate	[mm]
u	droplet velocity	[m/s]
$\bar{u}$	mean droplet velocity	[m/s]
z	axial coordinate	[mm]
α	spray angle	[-]
λ	wavelength of laser light	[nm]
ρ	density	[kg/m^3]
μ	viscosity	[Pa s]
σ	surface tension	[N/m]

subindices:

max	maximum
l	liquid
min	minimum
s	saturation
v	vapor

REFERENCES

1. **Dombrowski, N.& Johns, W.R.**, The aerodynamic instability and desintegration of viscous liquid sheets., *Chem. Eng. Science*, Vol. 18, 203–14, 1962.
2. **De Corso, S.M. & Kemeny, G.A.**, Effect of ambient and fuel pressure on nozzles spray angle., *Trans. ASME* 79, 605–615, 1957.
3. **De Corso, S.M.**, Effect of ambient and fuel pressure on spray drop size., *Trans. ASME, J. of Eng. for Power*, 10–18, January 1960.
4. **Dombrowski, N. & Hooper, P.C.**, The Effect of ambient density on drop formation in sprays., *Chem. Eng. Science*, Vol.17, 291–305, 1962.
5. **Mugele, R.A. & Evans, H.D.**, Droplet size distribution in sprays., *Ind. Eng. Chemistry*, Vol. 43, No. 6, 1317–24, 1951.
6. **Fraser, R.P. & Eisenklam, P.**, Liquid atomization and the drop size of sprays., *Trans. Instn. Chem. Engrs.*, Vol.34, 1956.
7. **Kim, K.Y. & Marshall, W.R., Jr.**, Drop-size distributions from pneumatic atomizers., *AIChE Journal*, Vol. 17, No. 3, 575–84,1971
8. **Dombrowski, N., & Wolfsohn, D.L.**, The atomization of water by swirl spray pressure nozzles., *Trans. Instn. Chem. Engrs.*, Vol. 50, 259–69, 1972.
9. **Azzopardi, B.J.**, Measurements of drop sizes., *Int. J. Heat and Mass Transfer*, Vol.22, 1245-1279, 1978.
10. **Durst, F. & Eliasson, B.**, Properties of laser-Doppler signals and their exploitation for particle size measurements., *Proc. of the LDA Symp.*, pp. 574–477, Copenhagen 1975.
11. **Swithenbank, J., Beer, J.M., Taylor, D.S. Abbot, D. & McGreath, C.G.**, A laser diagnostic technique for the mesurement of droplet and particle size distributions., *Prog. Astrn. Aeron.*, Vol. 53, No. 421, 1977.
12. **Yule, A.J., Chigier, N.A., Atakan, S. & Ungut, A.**, Particle size and velocity measurement by laser anemometry., *J. Energy*, Vol. 1, No. 4, 1977.
13. **Farmer, W.M.**, Visibility of large spheres observed with a laser velocimeter: a simple model., *Applied Optics* Vol. 19, No. 21, 1980.
14. **Bauckhage, K.**, Exploitation of laser-Doppler measurements for the characterization of nozzle sprays., *Preprints of the 1st World Congress "Particle Technology"* Part 1, pp. 223-33 Nürberg 1986.
15. **Bachalo, W.D. & Houser, M.H.**, An instrument for two component velocity and particle size measurement., *3rd Int. Symp. on Appl. Laser Anemometry to Fluid Mechanics*, 7.-9.6. 1986, Lisabon, Proc., 1986.
16. **Gabor, D.**, A new microscopic principle., *Nature*, Vol. 161, May 15, 777–778, 1948.
17. **Thompson, B.J.**, Holographic particle sizing techniques., *J. Physics E.*: Scientific Instruments, 7, 781–8, 1974.
18. **Trollinger, J.D.**, Particle field holography., *Optical Engineering*, 14, 383–92, 1975.
19. **Trollinger, J.D.**, Flow visualization holography., *Optical Engineering*, 14, 470–81, 1975.
20. **Hawighorst, A.**, Untersuchungen zur Tropfengrößenbestimung, Ph.D. Thesis, Universität Hannover, 1985.
21. **Timko, J.J.**, The investigation of transport phenomena by applied holography., *Proc. of the Int. Symposium on Flow Visualization*, pp. 429-34, Bochum 1980.
22. **Hariharan, P.**, *Optical holography*, Cambridge Univ. Press, 1984.
23. **Lee, S.Y. & Tankin, R.S.**, Study of liquid spray (water) in a condensable environment (steam), *Int. J. Heat and Mass Transfer*, Vol.27, No.3, 363 – 374, 1984.